

9-1-2012

# Vibration and buckling of composite beams using refined shear deformation

Thuc P. Vo

*Glyndwr University, [t.vo@glyndwr.ac.uk](mailto:t.vo@glyndwr.ac.uk)*

Huu-Tai Thai

*Hanyang University*

Follow this and additional works at: [http://epubs.glyndwr.ac.uk/aer\\_eng](http://epubs.glyndwr.ac.uk/aer_eng)



Part of the [Applied Mechanics Commons](#)

## Recommended Citation

Vo, T., Thai, H-T. (2012) "Vibration and buckling of composite beams using refined shear deformation Theory" *International Journal of Mechanical Sciences*, Volume 62, Issue 1, pp. 67-76

This Article is brought to you for free and open access by the Engineering at Glyndŵr University Research Online. It has been accepted for inclusion in Aeronautical Engineering by an authorized administrator of Glyndŵr University Research Online. For more information, please contact [d.jepson@glyndwr.ac.uk](mailto:d.jepson@glyndwr.ac.uk).

---

# Vibration and buckling of composite beams using refined shear deformation

## **Abstract**

Vibration and buckling analysis of composite beams with arbitrary lay-ups using refined shear deformation theory is presented. The theory accounts for the parabolical variation of shear strains through the depth of beam. Three governing equations of motion are derived from the Hamilton's principle. The resulting coupling is referred to as triply coupled vibration and buckling. A two-noded C1 beam element with five degree-of-freedom per node which accounts for shear deformation effects and all coupling coming from the material anisotropy is developed to solve the problem. Numerical results are obtained for composite beams to investigate effects of fiber orientation and modulus ratio on the natural frequencies, critical buckling loads and corresponding mode shapes.

## **Keywords**

Composite beams, refined shear deformation theory, triply coupled vibration and buckling

## **Disciplines**

Applied Mechanics | Engineering

## **Comments**

Copyright © 2012 Elsevier Ltd. All rights reserved. NOTICE: This is the author's version of a work that was accepted for publication in International Journal of Mechanical Sciences. Changes resulting from the publishing process, such as peer review, editing, corrections, structural formatting, and other quality control mechanisms, may not be reflected in this document. Changes may have been made to this work since it was submitted for publication. A definitive version was subsequently published in the International Journal of Mechanical Sciences, Volume 62, Issue 1, in 2012 located at <http://dx.doi.org/10.1016/j.ijmecsci.2012.06.001>

# Vibration and buckling of composite beams using refined shear deformation theory

Thuc P. Vo<sup>a,b,\*</sup>, Huu-Tai Thai<sup>c</sup>

<sup>a</sup>*School of Mechanical, Aeronautical and Electrical Engineering, Glyndŵr University, Mold Road, Wrexham LL11 2AW, UK.*

<sup>b</sup>*Advanced Composite Training and Development Centre, Unit 5, Hawarden Industrial Park Deeside, Flintshire CH5 3US, UK.*

<sup>c</sup>*Department of Civil and Environmental Engineering, Hanyang University, 17 Haengdang-dong, Seongdong-gu, Seoul 133-791, Republic of Korea.*

---

## Abstract

Vibration and buckling analysis of composite beams with arbitrary lay-ups using refined shear deformation theory is presented. The theory accounts for the parabolical variation of shear strains through the depth of beam. Three governing equations of motion are derived from the Hamilton's principle. The resulting coupling is referred to as triply coupled vibration and buckling. A two-noded  $C^1$  beam element with five degree-of-freedom per node which accounts for shear deformation effects and all coupling coming from the material anisotropy is developed to solve the problem. Numerical results are obtained for composite beams to investigate effects of fiber orientation and modulus ratio on the natural frequencies, critical buckling loads and corresponding mode shapes.

*Keywords:* Composite beams; refined shear deformation theory; triply coupled vibration and buckling.

---

## 1. Introduction

Structural components made with composite materials are increasingly being used in various engineering applications due to their attractive properties in strength, stiffness, and lightness. Understanding their dynamic and buckling behaviour is of increasing importance. The classical beam theory (CBT) known as Euler-Bernoulli beam theory is the simplest one and is applicable to slender beams only. For moderately deep beams, it overestimates buckling loads and natural frequencies due to ignoring the transverse shear effects. The first-order beam theory (FOBT) known as Timoshenko beam theory is proposed to overcome the limitations of the CBT by accounting for the transverse shear effects. Since the FOBT violates the zero shear stress conditions on the top and bottom surfaces of

---

\*Corresponding author, tel.: +44 1978 293979

Email address: [t.vo@glyndwr.ac.uk](mailto:t.vo@glyndwr.ac.uk) (Thuc P. Vo)

1 the beam, a shear correction factor is required to account for the discrepancy between the actual stress  
2 state and the assumed constant stress state. To remove the discrepancies in the CBT and FOBT,  
3 the higher-order beam theory (HOBT) is developed to avoid the use of shear correction factor and  
4 have a better prediction of response of laminated beams. The HOBTs can be developed based on  
5 the assumption of higher-order variations of in-plane displacement or both in-plane and transverse  
6 displacements through the depth of the beam. Many numerical techniques have been used to solve the  
7 dynamic and/or buckling analysis of composite beams using HOBTs. Some researchers studied the  
8 free vibration characteristics of composite beams by using finite element ([1]-[7]). Khdeir and Reddy  
9 ([8], [9]) developed analytical solutions for free vibration and buckling of cross-ply composite beams  
10 with arbitrary boundary conditions in conjunction with the state space approach. Analytical solutions  
11 were also derived by Kant et al. ([10], [11]) and Zhen and Wanji [12] to study vibration and buckling  
12 of composite beams. By using the method of power series expansion of displacement components,  
13 Matsunaga [13] analysed the natural frequencies and buckling stresses of composite beams. Aydogdu  
14 ([14]-[16]) carried out the vibration and buckling analysis of cross-ply and angle-ply with different sets  
15 of boundary conditions by using Ritz method. Jun et al. ([17],[18]) introduced the dynamic stiffness  
16 matrix method to solve the free vibration and buckling problems of axially loaded composite beams  
17 with arbitrary lay-ups.

18  
19 In this paper, which is extended from previous research [19], vibration and buckling analysis  
20 of composite beams using refined shear deformation theory is presented. [The displacement field](#)  
21 [is reduced from the so-called Refined Plate Theory developed by Shimpi \(\[20\], \[21\]\)](#) and based on  
22 the following assumptions: (1) the axial and transverse displacements consist of bending and shear  
23 components in which the bending components do not contribute toward shear forces and, likewise, the  
24 shear components do not contribute toward bending moments; (2) the bending component of axial  
25 displacement is similar to that given by the CBT; and (3) the shear component of axial displacement  
26 gives rise to the higher-order variation of shear strain and hence to shear stress through the depth of  
27 the beam in such a way that shear stress vanishes on the top and bottom surfaces. The most interesting  
28 feature of this theory is that it satisfies the zero traction boundary conditions on the top and bottom  
29 surfaces of the beam without using shear correction factors. The three governing equations of motion  
30 are derived from the Hamilton's principle. The resulting coupling is referred to as triply coupled  
31 vibration and buckling. A two-noded  $C^1$  beam element with five degree-of-freedom (DOF) per node  
32 which accounts for shear deformation effects and all coupling coming from the material anisotropy is  
33 developed to solve the problem. Numerical results are obtained for composite beams to investigate  
34 effects of fiber orientation and modulus ratio on the natural frequencies, critical buckling loads and  
35

1 corresponding mode shapes.  
 2  
 3

## 4 2. Kinematics

5  
 6  
 7 A laminated composite beam made of many plies of orthotropic materials in different orientations  
 8 with respect to the  $x$ -axis, as shown in Fig. 1, is considered. Based on the assumptions made in the  
 9 preceding section, the displacement field of the present theory can be obtained as:  
 10  
 11

$$12 \quad U(x, z, t) = u(x, t) - z \frac{\partial w_b(x, t)}{\partial x} + z \left[ \frac{1}{4} - \frac{5}{3} \left( \frac{z}{h} \right)^2 \right] \frac{\partial w_s(x, t)}{\partial x} \quad (1a)$$

$$13 \quad W(x, z, t) = w_b(x, t) + w_s(x, t) \quad (1b)$$

14  
 15  
 16  
 17  
 18 where  $u$  is the axial displacement along the mid-plane of the beam,  $w_b$  and  $w_s$  are the bending  
 19 and shear components of transverse displacement along the mid-plane of the beam, respectively. The  
 20 non-zero strains are given by:  
 21  
 22

$$23 \quad \epsilon_x = \frac{\partial U}{\partial x} = \epsilon_x^\circ + z \kappa_x^b + f \kappa_x^s \quad (2a)$$

$$24 \quad \gamma_{xz} = \frac{\partial W}{\partial x} + \frac{\partial U}{\partial z} = (1 - f') \gamma_{xz}^\circ = g \gamma_{xz}^\circ \quad (2b)$$

25  
 26  
 27  
 28  
 29 where

$$30 \quad f = z \left[ -\frac{1}{4} + \frac{5}{3} \left( \frac{z}{h} \right)^2 \right] \quad (3a)$$

$$31 \quad g = 1 - f' = \frac{5}{4} \left[ 1 - 4 \left( \frac{z}{h} \right)^2 \right] \quad (3b)$$

32  
 33  
 34  
 35  
 36  
 37 and  $\epsilon_x^\circ, \gamma_{xz}^\circ, \kappa_x^b, \kappa_x^s$  and  $\kappa_{xy}$  are the axial strain, shear strains and curvatures in the beam, respec-  
 38 tively defined as:  
 39  
 40

$$41 \quad \epsilon_x^\circ = u' \quad (4a)$$

$$42 \quad \gamma_{xz}^\circ = w_s' \quad (4b)$$

$$43 \quad \kappa_x^b = -w_b'' \quad (4c)$$

$$44 \quad \kappa_x^s = -w_s'' \quad (4d)$$

45  
 46  
 47  
 48  
 49  
 50 where differentiation with respect to the  $x$ -axis is denoted by primes ( $'$ ).  
 51  
 52

## 53 3. Variational Formulation

54  
 55  
 56 In order to derive the equations of motion, Hamilton's principle is used:  
 57

$$58 \quad \delta \int_{t_1}^{t_2} (\mathcal{K} - \mathcal{U} - \mathcal{V}) dt = 0 \quad (5)$$

where  $\mathcal{U}$  is the strain energy,  $\mathcal{V}$  is the potential energy, and  $\mathcal{K}$  is the kinetic energy.

The variation of the strain energy can be stated as:

$$\delta\mathcal{U} = \int_v (\sigma_x \delta\epsilon_x + \sigma_{xz} \delta\gamma_{xz}) dv = \int_0^l (N_x \delta\epsilon_z^\circ + M_x^b \delta\kappa_x^b + M_x^s \delta\kappa_x^s + Q_{xz} \delta\gamma_{xz}^\circ) dx \quad (6)$$

where  $N_x, M_x^b, M_x^s$  and  $Q_{xz}$  are the axial force, bending moments and shear force, respectively, defined by integrating over the cross-sectional area  $A$  as:

$$N_x = \int_A \sigma_x dA \quad (7a)$$

$$M_x^b = \int_A \sigma_x z dA \quad (7b)$$

$$M_x^s = \int_A \sigma_x f dA \quad (7c)$$

$$Q_{xz} = \int_A \sigma_{xz} g dA \quad (7d)$$

The variation of the potential energy of the axial force  $P_0$ , which is applied through the centroid, can be expressed as:

$$\delta\mathcal{V} = - \int_0^l P_0 [\delta w'_b (w'_b + w'_s) + \delta w'_s (w'_b + w'_s)] dx \quad (8)$$

The variation of the kinetic energy is obtained as:

$$\begin{aligned} \delta\mathcal{K} &= \int_v \rho_k (\dot{U} \delta\dot{U} + \dot{W} \delta\dot{W}) dv \\ &= \int_0^l \left[ \delta\dot{u} (m_0 \dot{u} - m_1 \dot{w}'_b - m_f \dot{w}'_s) + \delta\dot{w}_b m_0 (\dot{w}_b + \dot{w}_s) + \delta\dot{w}'_b (-m_1 \dot{u} + m_2 \dot{w}'_b + m_{fz} \dot{w}'_s) \right. \\ &\quad \left. + \delta\dot{w}_s m_0 (\dot{w}_b + \dot{w}_s) + \delta\dot{w}'_s (-m_f \dot{u} + m_{fz} \dot{w}'_b + m_{f2} \dot{w}'_s) \right] dx \end{aligned} \quad (9)$$

where the differentiation with respect to the time  $t$  is denoted by dot-superscript convention and  $\rho_k$  is the density of a  $k^{th}$  layer and  $m_0, m_1, m_2, m_f, m_{fz}$  and  $m_{f2}$  are the inertia coefficients, defined by:

$$m_f = -\frac{m_1}{4} + \frac{5}{3h^2} m_3 \quad (10a)$$

$$m_{fz} = -\frac{m_2}{4} + \frac{5}{3h^2} m_4 \quad (10b)$$

$$m_{f2} = \frac{m_2}{16} - \frac{5}{6h^2} m_4 + \frac{25}{9h^4} m_6 \quad (10c)$$

where:

$$(m_0, m_1, m_2, m_3, m_4, m_6) = \int_A \rho_k (1, z, z^2, z^3, z^4, z^6) dA \quad (11)$$

By substituting Eqs. (6), (8) and (9) into Eq. (5), the following weak statement is obtained:

$$\begin{aligned}
0 = & \int_{t_1}^{t_2} \int_0^l \left[ \delta \dot{u} (m_0 \dot{u} - m_1 \dot{w}_b' - m_f \dot{w}_s') + \delta \dot{w}_b m_0 (\dot{w}_b + \dot{w}_s) + \delta \dot{w}_b' (-m_1 \dot{u} + m_2 \dot{w}_b' + m_{fz} \dot{w}_s') \right. \\
& + \delta \dot{w}_s m_0 (\dot{w}_b + \dot{w}_s) + \delta \dot{w}_s' (-m_f \dot{u} + m_{fz} \dot{w}_b' + m_{f2} \dot{w}_s') \\
& \left. + P_0 [\delta w_b' (w_b' + w_s') + \delta w_s' (w_b' + w_s')] - N_x \delta u' + M_x^b \delta w_b'' + M_x^s \delta w_s'' - Q_{xz} \delta w_s' \right] dx dt \quad (12)
\end{aligned}$$

#### 4. Constitutive Equations

The stress-strain relations for the  $k^{th}$  lamina are given by:

$$\sigma_x = \bar{Q}_{11} \epsilon_x \quad (13a)$$

$$\sigma_{xz} = \bar{Q}_{55} \gamma_{xz} \quad (13b)$$

where  $\bar{Q}_{11}$  and  $\bar{Q}_{55}$  are the elastic stiffnesses transformed to the  $x$  direction. More detailed explanation can be found in Ref. [22].

The constitutive equations for bar forces and bar strains are obtained by using Eqs. (2), (7) and (13):

$$\begin{Bmatrix} N_x \\ M_x^b \\ M_x^s \\ Q_{xz} \end{Bmatrix} = \begin{bmatrix} R_{11} & R_{12} & R_{13} & 0 \\ & R_{22} & R_{23} & 0 \\ & & R_{33} & 0 \\ \text{sym.} & & & R_{44} \end{bmatrix} \begin{Bmatrix} \epsilon_x^\circ \\ \kappa_x^b \\ \kappa_x^s \\ \gamma_{xz}^\circ \end{Bmatrix} \quad (14)$$

where  $R_{ij}$  are the laminate stiffnesses of general composite beams and given by:

$$R_{11} = \int_y A_{11} dy \quad (15a)$$

$$R_{12} = \int_y B_{11} dy \quad (15b)$$

$$R_{13} = \int_y \left( -\frac{B_{11}}{4} + \frac{5}{3h^2} E_{11} \right) dy \quad (15c)$$

$$R_{22} = \int_y D_{11} dy \quad (15d)$$

$$R_{23} = \int_y \left( -\frac{D_{11}}{4} + \frac{5}{3h^2} F_{11} \right) dy \quad (15e)$$

$$R_{33} = \int_y \left( \frac{D_{11}}{16} - \frac{5}{6h^2} F_{11} + \frac{25}{9h^4} H_{11} \right) dy \quad (15f)$$

$$R_{44} = \int_y \left( \frac{25}{16} A_{55} - \frac{25}{2h^2} D_{55} + \frac{25}{h^4} F_{55} \right) dy \quad (15g)$$

where  $A_{ij}$ ,  $B_{ij}$  and  $D_{ij}$  matrices are the extensional, coupling and bending stiffness and  $E_{ij}$ ,  $F_{ij}$ ,  $H_{ij}$  matrices are the higher-order stiffnesses, respectively, defined by:

$$(A_{ij}, B_{ij}, D_{ij}, E_{ij}, F_{ij}, H_{ij}) = \int_z \bar{Q}_{ij}(1, z, z^2, z^3, z^4, z^6) dz \quad (16)$$

## 5. Governing equations of motion

The equilibrium equations of the present study can be obtained by integrating the derivatives of the varied quantities by parts and collecting the coefficients of  $\delta u$ ,  $\delta w_b$  and  $\delta w_s$ :

$$N'_x = m_0 \ddot{u} - m_1 \ddot{w}_b' - m_f \ddot{w}_s' \quad (17a)$$

$$M_x^{b''} - P_0(w_b'' + w_s'') = m_0(\ddot{w}_b + \ddot{w}_s) + m_1 \ddot{u}' - m_2 \ddot{w}_b'' - m_{fz} \ddot{w}_s'' \quad (17b)$$

$$M_x^{s''} + Q'_{xz} - P_0(w_b'' + w_s'') = m_0(\ddot{w}_b + \ddot{w}_s) + m_f \ddot{u}' - m_{fz} \ddot{w}_b'' - m_{f2} \ddot{w}_s'' \quad (17c)$$

The natural boundary conditions are of the form:

$$\delta u : N_x \quad (18a)$$

$$\delta w_b : M_x^{b'} - P_0(w_b' + w_s') - m_1 \ddot{u} + m_2 \ddot{w}_b' + m_{fz} \ddot{w}_s' \quad (18b)$$

$$\delta w_b' : M_x^b \quad (18c)$$

$$\delta w_s : M_x^{s'} + Q_{xz} - P_0(w_b' + w_s') - m_f \ddot{u} + m_{fz} \ddot{w}_b' + m_{f2} \ddot{w}_s' \quad (18d)$$

$$\delta w_s' : M_x^s \quad (18e)$$

By substituting Eqs. (4) and (14) into Eq. (17), the explicit form of the governing equations of motion can be expressed with respect to the laminate stiffnesses  $R_{ij}$ :

$$R_{11}u'' - R_{12}w_b''' - R_{13}w_s''' = m_0 \ddot{u} - m_1 \ddot{w}_b' - m_f \ddot{w}_s' \quad (19a)$$

$$R_{12}u''' - R_{22}w_b^{iv} - R_{23}w_s^{iv} - P_0(w_b'' + w_s'') = m_0(\ddot{w}_b + \ddot{w}_s) + m_1 \ddot{u}' - m_2 \ddot{w}_b'' - m_{fz} \ddot{w}_s'' \quad (19b)$$

$$R_{13}u''' - R_{23}w_b^{iv} - R_{33}w_s^{iv} + R_{44}w_s'' - P_0(w_b'' + w_s'') = m_0(\ddot{w}_b + \ddot{w}_s) + m_f \ddot{u}' - m_{fz} \ddot{w}_b'' - m_{f2} \ddot{w}_s'' \quad (19c)$$

Eq. (19) is the most general form for vibration and buckling of composite beams of composite beams, and the dependent variables,  $u$ ,  $w_b$  and  $w_s$  are fully coupled. The resulting coupling is referred to as triply axial-flexural coupled vibration and buckling. It can be seen that the explicit solutions for vibration and buckling of composite beams become complicated due to this triply coupling effect.



## 6. Finite Element Formulation

The present theory for composite beams described in the previous section is implemented via a displacement based finite element method. The variational statement in Eq. (12) requires that the bending and shear components of transverse displacement  $w_b$  and  $w_s$  be twice differentiable and  $C^1$ -continuous, whereas the axial displacement  $u$  must be only once differentiable and  $C^0$ -continuous. The generalized displacements are expressed over each element as a combination of the linear interpolation function  $\Psi_j$  for  $u$  and Hermite-cubic interpolation function  $\widehat{\psi}_j$  for  $w_b$  and  $w_s$  associated with node  $j$  and the nodal values:

$$u = \sum_{j=1}^2 u_j \Psi_j \quad (20a)$$

$$w_b = \sum_{j=1}^4 w_{bj} \widehat{\psi}_j \quad (20b)$$

$$w_s = \sum_{j=1}^4 w_{sj} \widehat{\psi}_j \quad (20c)$$

Substituting these expressions in Eq. (20) into the corresponding weak statement in Eq. (12), the finite element model of a typical element can be expressed as the standard eigenvalue problem:

$$([K] - P_0[G] - \omega^2[M])\{\Delta\} = \{0\} \quad (21)$$

where  $[K]$ ,  $[G]$  and  $[M]$  are the element stiffness matrix, the element geometric stiffness matrix and the element mass matrix, respectively. The explicit forms of  $[K]$  can be found in Ref. [19] and of  $[G]$  and  $[M]$  are given by:

$$G_{ij}^{22} = \int_0^l \psi'_i \psi'_j dz \quad (22a)$$

$$G_{ij}^{23} = \int_0^l \psi'_i \psi'_j dz \quad (22b)$$

$$G_{ij}^{33} = \int_0^l \psi'_i \psi'_j dz \quad (22c)$$

$$M_{ij}^{11} = \int_0^l m_0 \Psi_i \Psi_j dz \quad (22d)$$

$$M_{ij}^{12} = - \int_0^l m_1 \Psi_i \psi'_j dz \quad (22e)$$

$$M_{ij}^{13} = - \int_0^l m_f \Psi_i \psi'_j dz \quad (22f)$$

$$M_{ij}^{22} = \int_0^l m_0 \psi_i \psi_j + m_2 \psi'_i \psi'_j dz \quad (22g)$$

$$M_{ij}^{23} = \int_0^l m_0 \psi_i \psi_j + m_{fz} \psi'_i \psi'_j dz \quad (22h)$$

$$M_{ij}^{33} = \int_0^l m_0 \psi_i \psi_j + m_{f2} \psi'_i \psi'_j dz \quad (22i)$$

All other components are zero. In Eq.(21),  $\{\Delta\}$  is the eigenvector of nodal displacements corresponding to an eigenvalue:

$$\{\Delta\} = \{u \ w_b \ w_s\}^T \quad (23)$$

## 7. Numerical Examples

In this section, a number of numerical examples are presented and analysed for verification the accuracy of the present theory and investigation the natural frequencies, critical buckling loads and corresponding mode shapes of composite beams with arbitrary lay-ups. The boundary conditions of beam are presented by C for clamped edge:  $u = w_b = w'_b = w_s = w'_s = 0$ , S for simply-supported edge:  $u = w_b = w_s = 0$  and F for free edge. All laminate are of equal thickness and made of the same orthotropic material, whose properties are as follows:

Material I [3]:

$$E_1 = 241.5\text{GPa}, E_2 = 18.98\text{GPa}, G_{12} = G_{13} = 5.18\text{GPa}, G_{23} = 3.45\text{GPa}, \nu_{12} = 0.24, \rho = 2015\text{kg/m}^3 \quad (24)$$

Material II ([8], [9], [14], [15]):

$$E_1/E_2 = \text{open}, G_{12} = G_{13} = 0.6E_2, G_{23} = 0.5E_2, \nu_{12} = 0.25 \quad (25)$$

Material III ([14], [15]):

$$E_1/E_2 = \text{open}, G_{12} = G_{13} = 0.5E_2, G_{23} = 0.2E_2, \nu_{12} = 0.25 \quad (26)$$

Material IV [23]:

$$E_1 = 144.9\text{GPa}, E_2 = 9.65\text{GPa}, G_{12} = G_{13} = 4.14\text{GPa}, G_{23} = 3.45\text{GPa}, \nu_{12} = 0.3, \rho = 1389\text{kg/m}^3 \quad (27)$$

For convenience, the following non-dimensional terms are used in presenting the numerical results:

$$\bar{P}_{cr} = \begin{cases} \frac{P_{cr}L^2}{E_2bh^3} & \text{for Material II and III} \\ \frac{P_{cr}L^2}{E_1bh^3} & \text{for Material IV} \end{cases} \quad (28a)$$

$$\bar{\omega} = \begin{cases} \frac{\omega L^2}{h} \sqrt{\frac{\rho}{E_2}} & \text{for Material II and III} \\ \frac{\omega L^2}{h} \sqrt{\frac{\rho}{E_1}} & \text{for Material IV} \end{cases} \quad (28b)$$

1 As the first example, simply-supported symmetric cross-ply  $[90^\circ/0^\circ/0^\circ/90^\circ]$  composite beams with  
2 two span-to-height ratios ( $L/h = 2.273$  and  $22.73$ ) are considered. The material properties are assumed  
3 to be Material I. The first five natural frequencies are tabulated in Table 1 along with numerical results  
4 of previous studies ([3], [7], [18]). The ABAQUS solutions given in Ref. [3] were obtained by using  
5 the plane stress element type CPS8 (quadrilateral element of eight node, 16 DOF per element). The  
6 differences between the natural frequencies calculated by the present formulation and those using  
7 different higher-order beam theories are very small.  
8  
9

10 In the next example, vibration and buckling analysis of simply-supported composite beams with  
11 with symmetric cross-ply  $[0^\circ/90^\circ/0^\circ]$  and anti-symmetric cross-ply  $[0^\circ/90^\circ]$  lay-ups is performed. Ma-  
12 terial II and III with  $E_1/E_2 = 10$  and  $40$  are used. The fundamental natural frequencies and critical  
13 buckling loads for different span-to-height ratios are compared with exact solutions ([8], [9]) and the  
14 finite elements results ([5], [14], [15]) in Tables 2 and 3. In the case of the FOBT, a value of  $5/6$  is  
15 used for the shear correction factor. An excellent agreement between the predictions of the present  
16 model and the results of the other models mentioned (FOBT and HOBT) can be observed. Mate-  
17 rial II with  $E_1/E_2 = 40$  is chosen to show the effect of the axial force on the fundamental natural  
18 frequencies of beam with various  $L/h$  ratios (Fig. 2). It can be seen that the change of the natural  
19 frequency due to the axial force is noticeable. The natural frequency diminishes when the axial force  
20 changes from tensile to compressive, as expected. It is obvious that the natural frequency decreases  
21 with the increase of axial force, and the decrease becomes more quickly when the axial force is close to  
22 critical buckling load. For an anti-symmetric cross-ply lay-up, with  $L/h = 5, 10$  and  $20$ , at about  $P =$   
23  $3.903, 4.936$  and  $5.290$ , respectively, the natural frequencies become zero which implies that at these  
24 loads, bucklings occur as a degenerate case of natural vibration at zero frequency. It also means that  
25 the buckling loads of composite beams under the axial force can be also obtained indirectly through  
26 vibration problem by increasing the axial force until the corresponding natural frequency vanishes. In  
27 order to show the effect of material anisotropy ( $E_1/E_2$ ) on the critical buckling loads and the first  
28 four natural frequencies of a symmetric and an anti-symmetric cross-ply lay-up, a simply-supported  
29 composite beam with  $L/h = 5$  is performed. It is observed that the critical buckling loads and natural  
30 frequencies increase with increasing orthotropy (Figs. 3 and 4). For a symmetric cross-ply lay-up, as  
31 ratio of  $E_1/E_2$  increases, the order of the second and third vibration mode as well as the third and  
32 fourth vibration mode changes each other at  $E_1/E_2 = 7$  and  $27$ , respectively (Fig. 4).  
33  
34  
35  
36  
37  
38  
39  
40  
41  
42  
43  
44  
45  
46  
47  
48  
49  
50  
51  
52

53 To demonstrate the accuracy and validity of this study further, the fundamental natural frequencies  
54 of symmetric angle-ply  $[\theta/-\theta]_s$  composite beams are given in Table 4 to illustrate the effect of boundary  
55 conditions and of fiber orientation. In the following examples, Material IV with  $L/h = 15$  is used.  
56  
57  
58  
59  
60  
61  
62  
63  
64  
65

1 Variation of the critical buckling loads with respect to the fiber angle change is plotted in Fig. 5. The  
2 natural frequencies and buckling loads decrease monotonically with the increase of the fiber angle for  
3 all the boundary conditions considered. As the fiber angle increases, the buckling loads decrease more  
4 quickly than natural frequencies. For instant, the ratio between the buckling load at the fiber angle  $0^\circ$   
5 and  $90^\circ$  is 9.8 and similar value for natural frequency is 3.0 for clamped-clamped boundary condition.  
6 It is observed that the present results are in good agreement with previous studies ([16], [23], [24],  
7 [25]) for all fiber angles.  
8  
9

10 In order to investigate the effects of fiber orientation on the natural frequencies, critical buckling  
11 loads and corresponding mode shapes, a simply-supported anti-symmetric angle-ply  $[\theta/-\theta]$  composite  
12 beam is considered. The first four natural frequencies and critical buckling loads with respect to the  
13 fiber angle change are shown in Table 5 and Fig. 6. The uncoupled solution, which neglects the  
14 coupling effects coming from the material anisotropy, is also given. Due to coupling effects, the  
15 uncoupled solution might not be accurate. However, as the fiber angle increases, these effects become  
16 negligible. Therefore, it can be seen in Table 5 and Fig. 6 that the results by uncoupled and coupled  
17 solution are identical. For all fiber angles, the first four natural frequencies by the coupled solution  
18 exactly correspond to the first, second, third and fourth flexural mode by the uncoupled solution,  
19 respectively. It can be explained partly by the typical vibration mode shapes with the fiber angle  
20  $\theta = 45^\circ$  in Fig. 7. All the vibration modes exhibit double coupling (bending and shear components).  
21 It is indicated that the uncoupled solution is sufficiently accurate for an anti-symmetric angle-ply  
22 lay-up.  
23  
24  
25  
26  
27  
28  
29  
30  
31  
32  
33  
34  
35  
36

37 To investigate the coupling effects further, a clamped-clamped unsymmetric  $[0^\circ/\theta]$  composite beam  
38 is chosen. As the fiber angle increases, major effects of coupling on the natural frequencies and  
39 critical buckling loads are seen in Table 6 and Fig. 8. The uncoupled and coupled solution shows  
40 discrepancy indicating the coupling effects become significant, especially at the higher fiber angles.  
41 The typical vibration mode shapes corresponding to the first four natural frequencies with the fiber  
42 angle  $\theta = 60^\circ$  are illustrated in Fig. 9. The buckling mode shapes with various fiber angles  $\theta =$   
43  $30^\circ, 60^\circ$  and  $90^\circ$  are also given in Fig. 10. Relative measures of the axial and flexural displacements  
44 show that all the vibration and buckling modes are triply coupled mode (axial, bending and shear  
45 components). This fact explains as the fiber angle changes, the uncoupled solution disagrees with  
46 coupled solution as anisotropy of the beam gets higher. That is, the uncoupled solution is no longer  
47 valid for unsymmetrically laminated composite beams, and triply extension-bending-shear coupled  
48 vibration and buckling should be considered simultaneously for accurate analysis of composite beams.  
49  
50  
51  
52  
53  
54  
55  
56  
57  
58  
59  
60  
61  
62  
63  
64  
65

## 8. Conclusions

A two-noded  $C^1$  beam element of five degree-of-freedom per node is developed to study the vibration and buckling behaviour of composite beams using refined shear deformation theory. This model is capable of predicting accurately the natural frequencies, critical buckling loads and corresponding mode shapes. It accounts for the parabolical variation of shear strains through the depth of the beam, and satisfies the zero traction boundary conditions on the top and bottom surfaces of the beam without using shear correction factor. The uncoupled solution is accurate for lower degrees of material anisotropy, but, becomes inappropriate as the anisotropy of the beam gets higher, and triply extension-bending-shear coupled vibration and buckling should be considered simultaneously for accurate analysis of composite beams. The present model is found to be appropriate and efficient in analyzing vibration and buckling problem of composite beams.

## 9. References

### References

- [1] K. Chandrashekhara, K. Bangera, Free vibration of composite beams using a refined shear flexible beam element, *Computers and Structures* 43 (4) (1992) 719 – 727.
- [2] S. R. Marur, T. Kant, Free vibration analysis of fiber reinforced composite beams using higher order theories and finite element modelling, *Journal of Sound and Vibration* 194 (3) (1996) 337 – 351.
- [3] M. Karama, B. A. Harb, S. Mistou, S. Caperaa, Bending, buckling and free vibration of laminated composite with a transverse shear stress continuity model, *Composites Part B: Engineering* 29 (3) (1998) 223 – 234.
- [4] G. Shi, K. Y. Lam, Finite element vibration analysis of composite beams based on higher-order beam theory, *Journal of Sound and Vibration* 219 (4) (1999) 707 – 721.
- [5] M. V. V. S. Murthy, D. R. Mahapatra, K. Badarinarayana, S. Gopalakrishnan, A refined higher order finite element for asymmetric composite beams, *Composite Structures* 67 (1) (2005) 27 – 35.
- [6] P. Subramanian, Dynamic analysis of laminated composite beams using higher order theories and finite elements, *Composite Structures* 73 (3) (2006) 342 – 353.

- 1 [7] P. Vidal, O. Polit, A family of sinus finite elements for the analysis of rectangular laminated  
2 beams, *Composite Structures* 84 (1) (2008) 56 – 72.  
3  
4
- 5 [8] A. A. Khdeir, J. N. Reddy, Free vibration of cross-ply laminated beams with arbitrary boundary  
6 conditions, *International Journal of Engineering Science* 32 (12) (1994) 1971–1980, cited By (since  
7 1996) 47.  
8  
9
- 10 [9] A. A. Khdeir, J. N. Reddy, Buckling of cross-ply laminated beams with arbitrary boundary  
11 conditions, *Composite Structures* 37 (1) (1997) 1 – 3.  
12  
13
- 14 [10] T. Kant, S. R. Marur, G. Rao, Analytical solution to the dynamic analysis of laminated beams  
15 using higher order refined theory, *Composite Structures* 40 (1) (1997) 1 – 9.  
16  
17
- 18 [11] T. Kant, K. Swaminathan, Analytical solutions for free vibration of laminated composite and  
19 sandwich plates based on a higher-order refined theory, *Composite Structures* 53 (1) (2001) 73 –  
20 85.  
21  
22
- 23 [12] W. Zhen, C. Wanji, An assessment of several displacement-based theories for the vibration and  
24 stability analysis of laminated composite and sandwich beams, *Composite Structures* 84 (4) (2008)  
25 337 – 349.  
26  
27
- 28 [13] H. Matsunaga, Vibration and buckling of multilayered composite beams according to higher order  
29 deformation theories, *Journal of Sound and Vibration* 246 (1) (2001) 47 – 62.  
30  
31
- 32 [14] M. Aydogdu, Vibration analysis of cross-ply laminated beams with general boundary conditions  
33 by Ritz method, *International Journal of Mechanical Sciences* 47 (11) (2005) 1740 – 1755.  
34  
35
- 36 [15] M. Aydogdu, Buckling analysis of cross-ply laminated beams with general boundary conditions  
37 by Ritz method, *Composites Science and Technology* 66 (10) (2006) 1248 – 1255.  
38  
39
- 40 [16] M. Aydogdu, Free vibration analysis of angle-ply laminated beams with general boundary condi-  
41 tions, *Journal of Reinforced Plastics and Composites* 25 (15) (2006) 1571–1583.  
42  
43
- 44 [17] L. Jun, L. Xiaobin, H. Hongxing, Free vibration analysis of third-order shear deformable compos-  
45 ite beams using dynamic stiffness method, *Archive of Applied Mechanics* 79 (2009) 1083–1098.  
46  
47
- 48 [18] L. Jun, H. Hongxing, Free vibration analyses of axially loaded laminated composite beams based  
49 on higher-order shear deformation theory, *Meccanica* 46 (2011) 1299–1317.  
50  
51
- 52 [19] T. P. Vo and H. T. Thai, Static behaviour of composite beams using various refined shear defor-  
53 mation theories. *Composite Structures* 94 (8) (2012) 2513–2522  
54  
55  
56  
57  
58  
59  
60  
61

- 1 [20] R. P. Shimpi, Refined plate theory and its variants, *AIAA Journal* 40 (1) (2002) 137–146  
2  
3  
4 [21] R. P. Shimpi, H. G. Patel, A two variable refined plate theory for orthotropic plate analysis,  
5 *International Journal of Solids and Structures* 43 (22-23) (2006) 6783–6799  
6  
7  
8 [22] R. M. Jones, *Mechanics of Composite Materials*, Taylor & Francis, 1999.  
9  
10 [23] K. Chandrashekhara, K. Krishnamurthy, S. Roy, Free vibration of composite beams including  
11 rotary inertia and shear deformation, *Composite Structures* 14 (4) (1990) 269 – 279.  
12  
13  
14 [24] S. Krishnaswamy, K. Chandrashekhara, W. Z. B. Wu, Analytical solutions to vibration of gener-  
15 ally layered composite beams, *Journal of Sound and Vibration* 159 (1) (1992) 85 – 99.  
16  
17  
18 [25] W. Q. Chen, C. F. Lv, Z. G. Bian, Free vibration analysis of generally laminated beams via  
19 state-space-based differential quadrature, *Composite Structures* 63 (3-4) (2004) 417 – 425.  
20  
21  
22  
23  
24  
25  
26  
27  
28  
29  
30  
31  
32  
33  
34  
35  
36  
37  
38  
39  
40  
41  
42  
43  
44  
45  
46  
47  
48  
49  
50  
51  
52  
53  
54  
55  
56  
57  
58  
59  
60  
61  
62  
63  
64  
65

1  
2  
3 Figure 1: Geometry of a laminated composite beam.  
4  
5  
6

7 Figure 2: The interaction diagram between non-dimensional critical buckling load and fundamental natural frequency of  
8 a simply supported symmetric and anti-symmetric cross-ply composite beam with  $L/h = 5, 10$  and  $20$ .  
9  
10

11  
12  
13 Figure 3: Effect of material anisotropy on the non-dimensional critical buckling loads of a simply supported symmetric  
14 and anti-symmetric cross-ply composite beam with  $L/h = 5$ .  
15  
16  
17

18  
19  
20 Figure 4: Effect of material anisotropy on the first five non-dimensional natural frequencies of a simply supported  
21 symmetric and anti-symmetric cross-ply composite beam with  $L/h = 5$ .  
22  
23  
24

25  
26 Figure 5: Variation of the non-dimensional critical buckling loads of symmetric angle-ply  $[\theta/-\theta]_s$  composite beams with  
27 respect to the fiber angle change.  
28  
29  
30

31  
32 Figure 6: Variation of the non-dimensional critical buckling loads of a simply-supported anti-symmetric angle-ply  $[\theta/-\theta]$   
33 composite beam with respect to the fiber angle change.  
34  
35  
36

37  
38 Figure 7: Vibration mode shapes of the axial and flexural components of a simply-supported composite beam with the  
39 fiber angle  $45^\circ$ .  
40  
41  
42

43  
44 Figure 8: Variation of the non-dimensional critical buckling loads of a clamped-clamped unsymmetric  $[0^\circ/\theta]$  composite  
45 beam with respect to the fiber angle change.  
46  
47  
48

49  
50 Figure 9: Vibration mode shapes with the axial and flexural components of a clamped-clamped composite beam with  
51 the fiber angle  $60^\circ$ .  
52  
53  
54

55  
56 Figure 10: Bucking mode shapes with the axial and flexural components of a clamped-clamped composite beam with  
57 the fiber angles  $30^\circ, 60^\circ$  and  $90^\circ$ .  
58  
59  
60  
61



1  
2  
3  
4  
5  
6  
7  
8  
9  
10  
11  
12  
13  
14  
15  
16  
17  
18  
19  
20  
21  
22  
23  
24  
25  
26  
27  
28  
29  
30  
31  
32  
33  
34  
35  
36  
37  
38  
39  
40  
41  
42  
43  
44  
45  
46  
47  
48  
49  
50  
51  
52  
53  
54  
55  
56  
57  
58  
59  
60  
61  
62  
63  
64  
65

Table 1: The first five fundamental natural frequencies (Hz) of simply-supported beams with a symmetric cross-ply  $[90^\circ/0^\circ/0^\circ/90^\circ]$  lay-up ( $L/h=2.273$  and  $22.73$ , Material I).

Table 2: Effect of span-to-height ratios on the non-dimensional fundamental natural frequencies of a symmetric and an anti-symmetric cross-ply composite beam with simply-supported boundary condition (Material II with  $E_1/E_2 = 40$ ).

Table 3: Effect of span-to-height ratios on the non-dimensional critical buckling loads of a symmetric and an anti-symmetric cross-ply composite beam with simply-supported boundary condition (Material II and III with  $E_1/E_2 = 10$  and  $40$ ).

Table 4: The non-dimensional fundamental frequencies of symmetric angle-ply  $[\theta/-\theta]_s$  composite beams with respect to the fiber angle change ( $L/h = 15$ , Material IV).

Table 5: The first four non-dimensional frequencies of anti-symmetric angle-ply  $[\theta/-\theta]$  composite beams with respect to the fiber angle change ( $L/h = 15$ , Material IV).

Table 6: The first four non-dimensional frequencies of unsymmetric  $[0^\circ/\theta]$  composite beams with respect to the fiber angle change ( $L/h = 15$ , Material IV).

**CAPTIONS OF TABLES**

Table 1: The first five natural frequencies (Hz) of simply-supported beams with a symmetric cross-ply  $[90^0 / 0^0 / 0^0 / 90^0]$  lay-up (Material I with  $L/h=2.273$  and  $22.73$ ).

Table 2: Effect of span-to-height ratios on the non-dimensional fundamental natural frequencies of a symmetric and an anti-symmetric cross-ply composite beam with simply-supported boundary condition (Material II with  $E_1/E_2 = 40$ ).

Table 3: Effect of span-to-height ratios on the non-dimensional critical buckling loads of a symmetric and an anti-symmetric cross-ply composite beam with simply-supported boundary condition (Material II and III with  $E_1/E_2 = 10$ ).

Table 4: Effect of span-to-height ratios on the non-dimensional critical buckling loads of a symmetric and an anti-symmetric cross-ply composite beam with simply-supported boundary condition (Material II and III with  $E_1/E_2 = 40$ ).

Table 5: The non-dimensional fundamental natural frequencies of symmetric angle-ply  $[\theta / -\theta]_s$  composite beams with respect to the fiber angle change (Material IV with  $L/h = 15$ ).

Table 6: The first four non-dimensional natural frequencies of a simply-supported anti-symmetric angle-ply  $[\theta / -\theta]$  composite beam with respect to the fiber angle change (Material IV with  $L/h = 15$ ).

Table 7: The first four non-dimensional natural frequencies of an unsymmetric  $[0 / \theta]$  clamped-clamped composite beam with respect to the fiber angle change (Material IV with  $L/h = 15$ ).

Table 1: The first five natural frequencies (Hz) of simply-supported beams with a symmetric cross-ply  $[90^0 / 0^0 / 0^0 / 90^0]$  lay-up (Material I with  $L/h=2.273$  and  $22.73$ ).

Mode	L/h = 2.273				L/h = 22.73				
	ABAQUS [3]	Ref. [3]	Ref. [7]	Present	ABAQUS [3]	Ref. [3]	Ref. [7]	Ref. [18]	Present
1	82.90	83.70	82.81	82.42	14.95	14.96	14.97	14.97	14.42
2	200.60	195.80	195.62	195.20	57.60	57.90	57.85	57.87	55.88
3	324.30	313.40	319.36	315.88	122.80	123.70	123.55	123.58	119.76
4	450.10	441.80	460.18	449.83	204.20	206.40	206.18	206.01	200.44
5	576.40	583.80	515.41	578.65	296.60	300.60	300.71	299.68	292.73

Table 2: Effect of span-to-height ratios on the non-dimensional fundamental natural frequencies of a symmetric and an anti-symmetric cross-ply composite beam with simply-supported boundary condition (Material II with  $E_1/E_2 = 40$ ).

Lay-ups	Theory	Reference	L/h			
			5	10	20	50
$[0^0/90^0/0^0]$	FOBT	Khdeir and Reddy [8]	9.205	13.670	-	-
		Present	9.205	13.665	16.359	17.456
	HOBT	Murthy et al. [5]	9.207	13.614	-	-
		Khdeir and Reddy [8]	9.208	13.614	-	-
		Aydogdu [14]	9.207	-	16.337	-
		Present	9.206	13.607	16.327	17.449
$[0^0/90^0]$	FOBT	Khdeir and Reddy [8]	5.953	6.886	-	-
		Present	5.886	6.848	7.187	7.294
	HOBT	Murthy et al. [5]	6.045	6.908	-	-
		Khdeir and Reddy [8]	6.128	6.945	-	-
		Aydogdu [14]	6.144	-	7.218	-
		Present	6.058	6.909	7.204	7.296

Table 3: Effect of span-to-height ratios on the non-dimensional critical buckling loads of a symmetric and an anti-symmetric cross-ply composite beam with simply-supported boundary condition (Material II and III with  $E_1/E_2 = 10$ ).

Lay-ups	Theory	Reference	L/h			
			5	10	20	50
<i>Material II</i>						
[0 <sup>0</sup> /90 <sup>0</sup> /0 <sup>0</sup> ]	FOBT	Present	4.752	6.805	7.630	7.897
	HOBT	Aydogdu [15]	4.726	-	7.666	-
		Present	4.709	6.778	7.620	7.896
[0 <sup>0</sup> /90 <sup>0</sup> ]	FOBT	Present	1.883	2.148	2.226	2.249
	HOBT	Aydogdu [15]	1.919	-	2.241	-
		Present	1.910	2.156	2.228	2.249
<i>Material III</i>						
[0 <sup>0</sup> /90 <sup>0</sup> /0 <sup>0</sup> ]	FOBT	Present	4.069	6.420	7.503	7.875
	HOBT	Aydogdu [15]	3.728	-	7.459	-
		Present	3.717	6.176	7.416	7.860
[0 <sup>0</sup> /90 <sup>0</sup> ]	FOBT	Present	1.605	1.876	1.958	1.983
	HOBT	Aydogdu [15]	1.765	-	2.226	-
		Present	1.758	2.104	2.214	2.247

Table 4: Effect of span-to-height ratios on the non-dimensional critical buckling loads of a symmetric and an anti-symmetric cross-ply composite beam with simply-supported boundary condition (Material II and III with  $E_1/E_2 = 40$ ).

Lay-ups	Theory	Reference	L/h			
			5	10	20	50
<i>Material II</i>						
[0 <sup>0</sup> /90 <sup>0</sup> /0 <sup>0</sup> ]	FOBT	Khdeir and Reddy [9]	8.606	18.989	-	-
		Present	8.604	18.974	27.154	30.882
	HOBT	Khdeir and Reddy [9]	8.613	18.832	-	-
		Aydogdu [15]	8.613	-	27.084	-
		Present	8.609	18.814	27.050	30.859
		Present	3.680	4.848	5.265	5.395
[0 <sup>0</sup> /90 <sup>0</sup> ]	FOBT	Present	3.680	4.848	5.265	5.395
	HOBT	Aydogdu [15]	3.906	-	5.296	-
		Present	3.903	4.936	5.290	5.399
<i>Material III</i>						
[0 <sup>0</sup> /90 <sup>0</sup> /0 <sup>0</sup> ]	FOBT	Present	6.600	16.253	25.620	30.549
	HOBT	Aydogdu [15]	5.896	-	24.685	-
		Present	5.895	14.857	24.655	30.319
[0 <sup>0</sup> /90 <sup>0</sup> ]	FOBT	Present	3.110	4.571	5.180	5.381
	HOBT	Aydogdu [15]	3.376	-	5.225	-
		Present	3.373	4.697	5.219	5.387

Table 5: The non-dimensional fundamental natural frequencies of symmetric angle-ply  $[\theta/-\theta]_s$  composite beams with respect to the fiber angle change (Material IV with  $L/h = 15$ ).

Boundary conditions	Reference	Fiber angle $\theta$						
		$0^0$	$15^0$	$30^0$	$45^0$	$60^0$	$75^0$	$90^0$
CC	Aydogdu [16]	4.9730	4.2940	2.1950	1.9290	1.6690	1.6120	1.6190
	Chandrashekhara et al. [23]	4.8487	4.6635	4.0981	3.1843	2.1984	1.6815	1.6200
	Krishnaswamy et al. [24]	4.8690	3.9880	2.8780	1.9470	1.6690	1.6120	1.6190
	Chen et al. [25]	4.8575	3.6484	2.3445	1.8383	1.6711	1.6161	1.6237
	Present	4.8969	4.5695	3.2355	1.9918	1.6309	1.6056	1.6152
SS	Aydogdu [16]	2.6510	1.8960	1.1410	0.8040	0.7360	0.7250	0.7290
	Chandrashekhara et al. [23]	2.6560	2.5105	2.1032	1.5368	1.0124	0.7611	0.7320
	Present	2.6494	2.4039	1.5540	0.9078	0.7361	0.7247	0.7295
CF	Aydogdu [16]	0.9810	0.6760	0.4140	0.2880	0.2620	0.2580	0.2600
	Chandrashekhara et al. [23]	0.9820	0.9249	0.7678	0.5551	0.3631	0.2723	0.2619
	Present	0.9801	0.8836	0.5614	0.3253	0.2634	0.2593	0.2611
CS	Aydogdu [16]	3.7750	2.9600	1.6710	1.1780	1.1500	1.1220	1.1290
	Chandrashekhara et al. [23]	3.7310	3.5590	3.0570	2.3030	1.5510	1.1750	1.1360
	Krishnaswamy et al. [24]	3.8370	3.2430	2.2130	1.3880	1.1460	1.1290	1.1310
	Present	3.8183	3.5079	2.3538	1.4019	1.1407	1.1231	1.1302

Table 6: The first four non-dimensional natural frequencies of a simply-supported anti-symmetric angle-ply  $[\theta / -\theta]$  composite beam with respect to the fiber angle change (Material IV with  $L/h = 15$ ).

Fiber angle	No coupling				With coupling			
	$\omega_{z_1}$	$\omega_{z_2}$	$\omega_{z_3}$	$\omega_{z_4}$	$\omega_1$	$\omega_2$	$\omega_3$	$\omega_4$
$0^0$	2.6494	8.9572	16.6431	24.7032	2.6494	8.9572	16.6431	24.7032
$15^0$	2.4039	8.3223	15.7685	23.7045	2.4039	8.3223	15.7685	23.7045
$30^0$	1.5540	5.7944	11.8313	18.8714	1.5540	5.7944	11.8313	18.8714
$45^0$	0.9078	3.5255	7.5850	12.7587	0.9078	3.5255	7.5850	12.7587
$60^0$	0.7361	2.8798	6.2616	10.6606	0.7361	2.8798	6.2616	10.6606
$75^0$	0.7247	2.8352	6.1639	10.4930	0.7247	2.8352	6.1639	10.4930
$90^0$	0.7295	2.8526	6.1977	10.5426	0.7295	2.8526	6.1977	10.5426



Table 7: The first four non-dimensional natural frequencies of an unsymmetric  $[0/\theta]$  clamped-clamped composite beam with respect to the fiber angle change (Material IV with  $L/h = 15$ ).

Fiber angle	No coupling				With coupling			
	$\omega_{z_1}$	$\omega_{z_2}$	$\omega_{z_3}$	$\omega_{z_4}$	$\omega_1$	$\omega_2$	$\omega_3$	$\omega_4$
$0^0$	4.897	11.493	18.400	26.448	4.897	11.493	18.400	26.448
$15^0$	4.742	11.212	18.037	26.011	4.730	11.192	18.015	25.988
$30^0$	4.272	10.330	16.901	24.637	3.957	9.744	16.218	23.893
$45^0$	4.009	9.802	16.192	23.743	3.108	7.967	13.886	21.042
$60^0$	3.950	9.665	15.977	23.437	2.859	7.400	13.071	19.975
$75^0$	3.938	9.625	15.896	23.306	2.840	7.351	12.984	19.841
$90^0$	3.935	9.615	15.872	23.264	2.846	7.361	12.992	19.844

## CAPTIONS OF FIGURES

Figure 1: Geometry of a laminated composite beam.

Figure 2: The interaction diagram between non-dimensional critical buckling load and fundamental natural frequency of a symmetric and an anti-symmetric cross-ply composite beam with simply-supported boundary condition (Material II with  $L/h = 5, 10$  and  $20$ ).

Figure 3: Effect of material anisotropy on the non-dimensional critical buckling loads of a symmetric and an anti-symmetric cross-ply composite beam with simply-supported boundary condition (Material II with  $L/h = 5$ ).

Figure 4: Effect of material anisotropy on the first four non-dimensional natural frequencies of a symmetric and an anti-symmetric cross-ply composite beam with simply-supported boundary condition (Material II with  $L/h = 5$ ).

Figure 5: Variation of the non-dimensional critical buckling loads of symmetric angle-ply  $[\theta/-\theta]_s$  composite beams with respect to the fiber angle change (Material IV with  $L/h = 15$ ).

Figure 6: Variation of the non-dimensional critical buckling loads of a simply-supported anti-symmetric angle-ply  $[\theta/-\theta]$  composite beam with respect to the fiber angle change (Material IV with  $L/h = 15$ ).

Figure 7: Vibration mode shapes with the axial and flexural components of a simply-supported composite beam with the fiber angle  $45^0$

Figure 8: Variation of the non-dimensional critical buckling loads of a clamped-clamped unsymmetric  $[0/\theta]$  composite beam with respect to the fiber angle change (Material IV with  $L/h = 15$ ).

Figure 9: Vibration mode shapes with the axial and flexural components of a clamped-clamped composite beam with the fiber angle  $60^0$ .

Figure 10: Bucking mode shapes with the axial and flexural components of a clamped-clamped composite beam with the fiber angles  $30^0, 60^0$  and  $90^0$ .

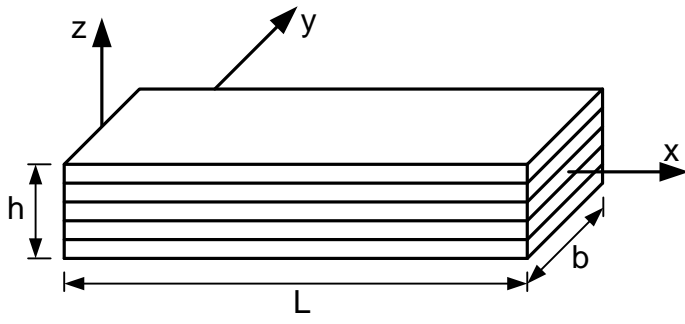
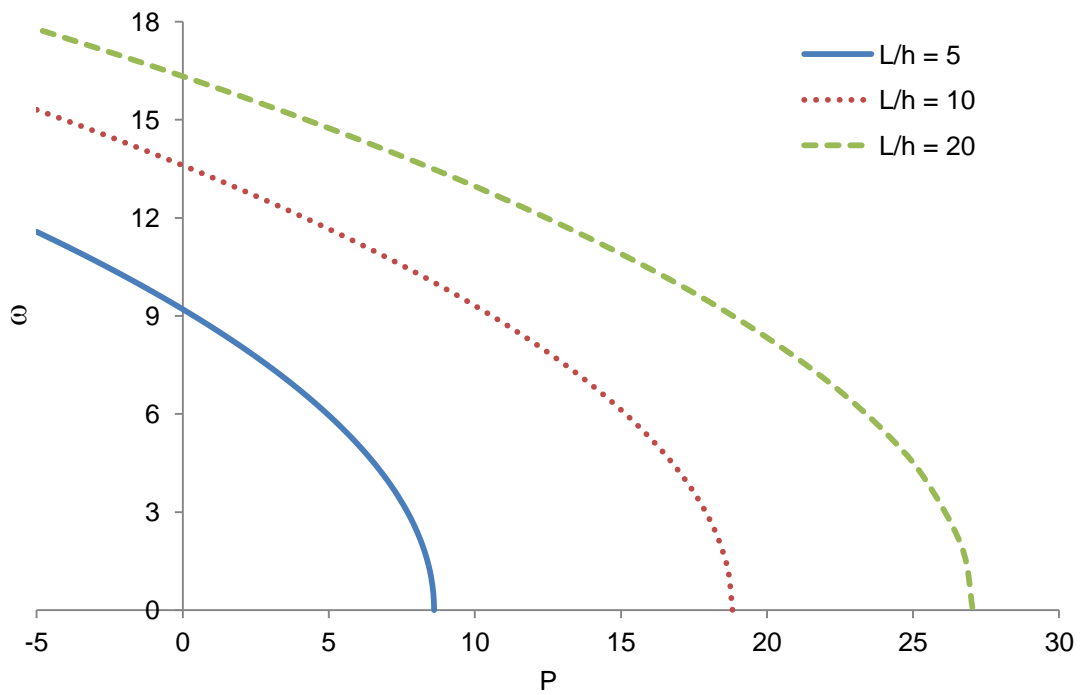
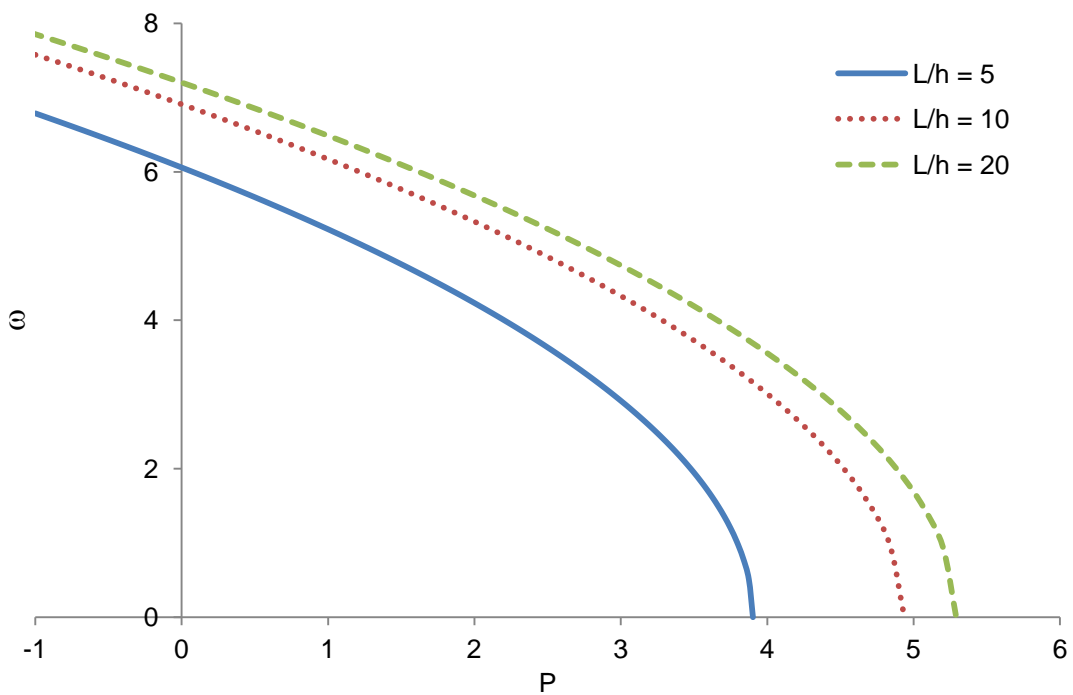


Figure 1: Geometry of a laminated composite beam.



a. Symmetric cross-ply lay-up ( $[0^0/90^0/0^0]$ )



b. Anti-symmetric cross-ply lay-up ( $[0^0/90^0]$ )

Figure 2: The interaction diagram between non-dimensional critical buckling load and fundamental natural frequency of a symmetric and an anti-symmetric cross-ply composite beam with simply-supported boundary condition (Material II with  $L/h = 5, 10$  and  $20$ ).

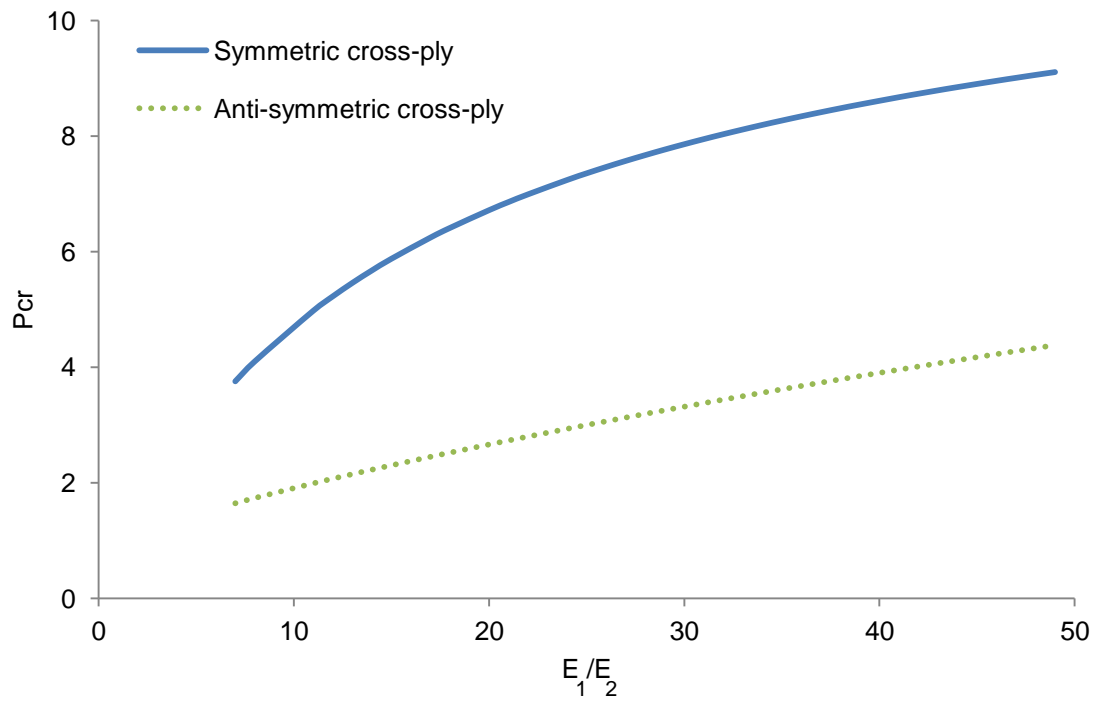
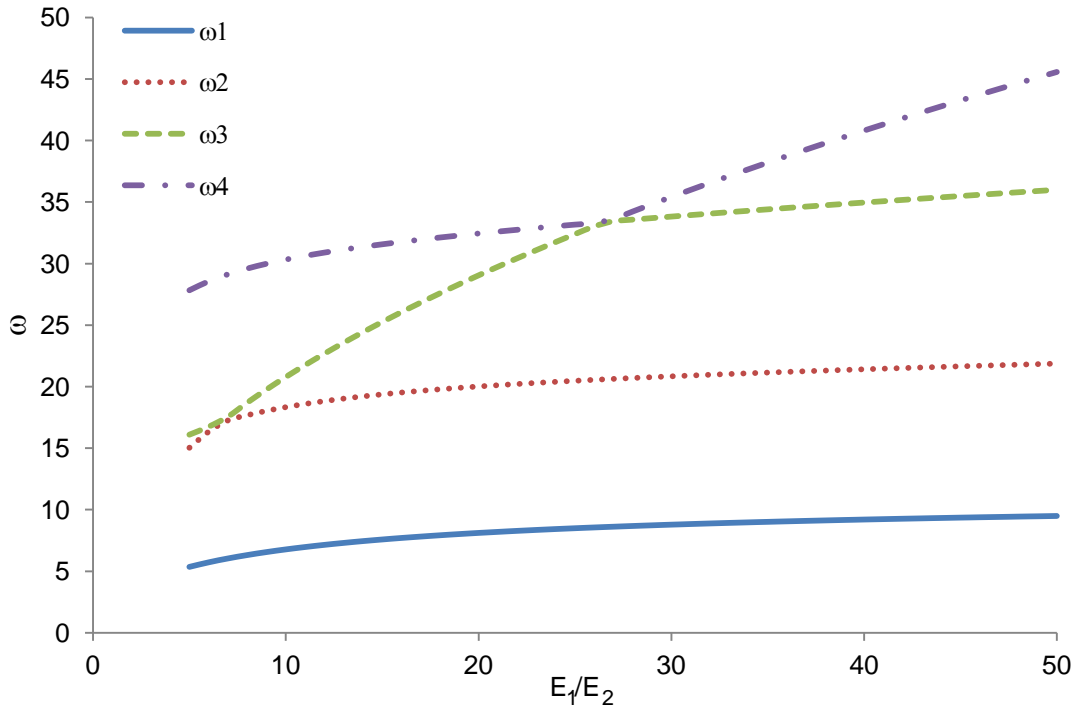
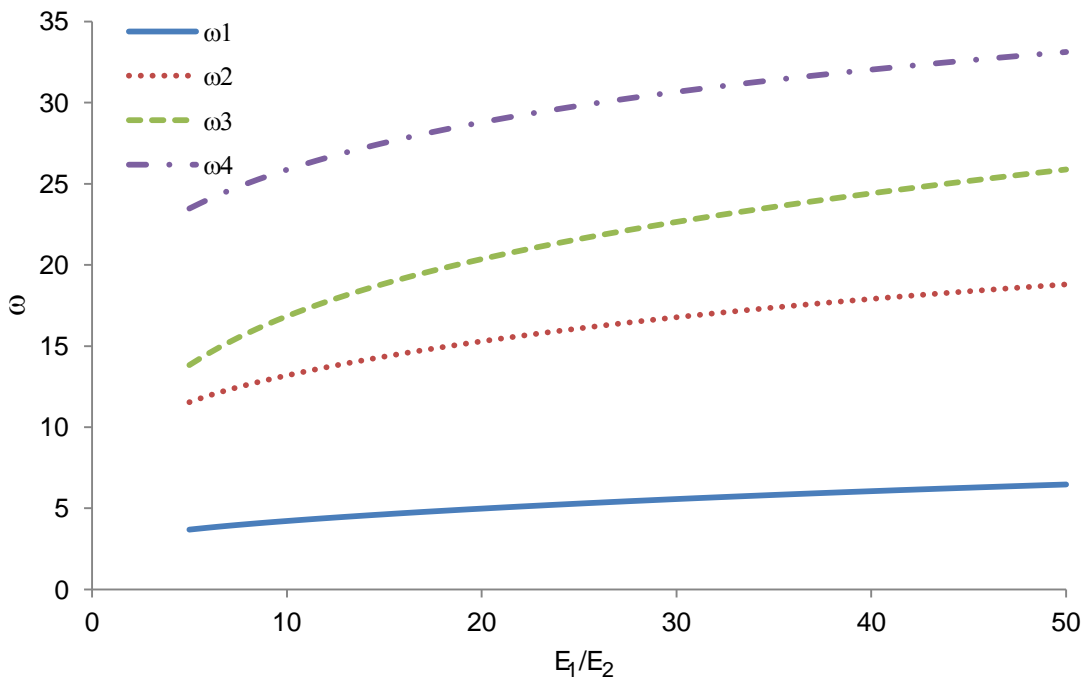


Figure 3: Effect of material anisotropy on the non-dimensional critical buckling loads of a symmetric and an anti-symmetric cross-ply composite beam with simply-supported boundary condition (Material II with  $L/h = 5$ ).



a. Symmetric cross-ply lay-up ( $[0^0/90^0/0^0]$ )



b. Anti-symmetric cross-ply lay-up ( $[0^0/90^0]$ )

Figure 4: Effect of material anisotropy on the first four non-dimensional natural frequencies of a symmetric and an anti-symmetric cross-ply composite beam with simply-supported boundary condition (Material II with  $L/h = 5$ ).

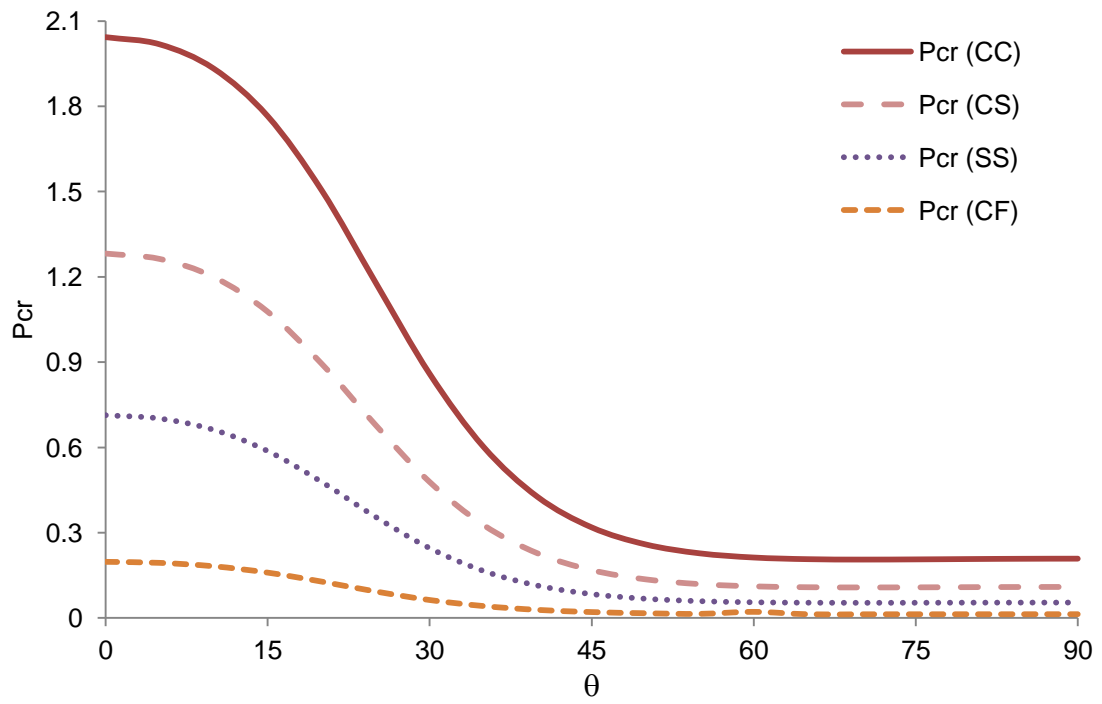


Figure 5: Variation of the non-dimensional critical buckling loads of symmetric angle-ply  $[\theta / -\theta]_s$  composite beams with respect to the fiber angle change (Material IV with  $L/h = 15$ ).

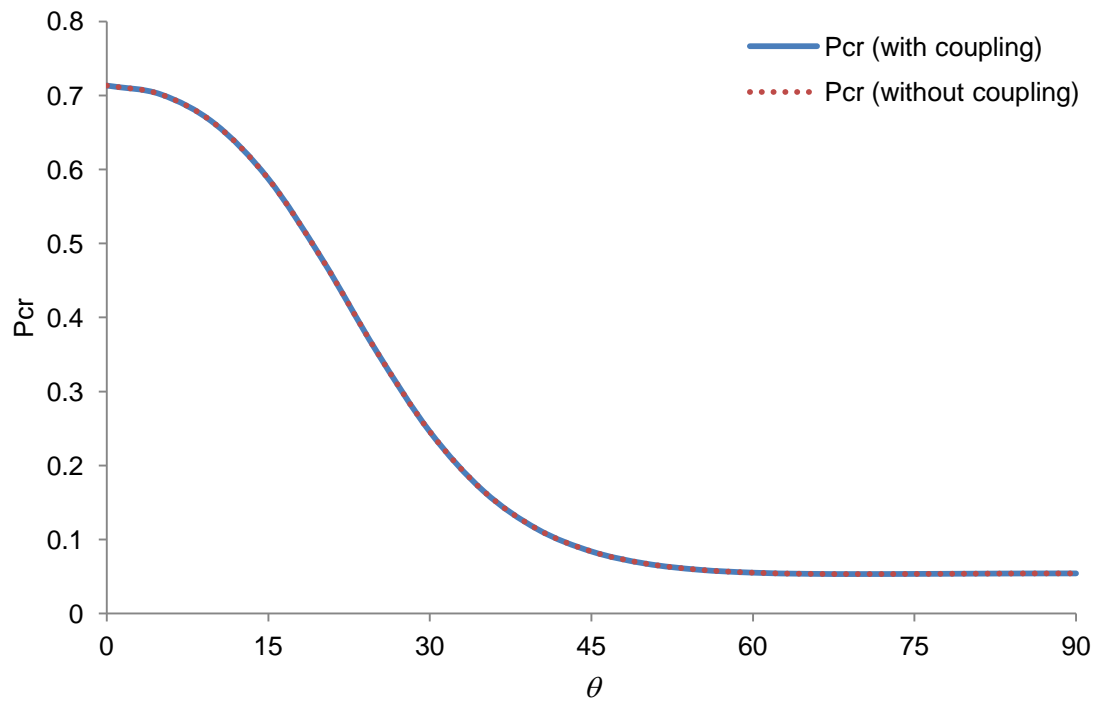
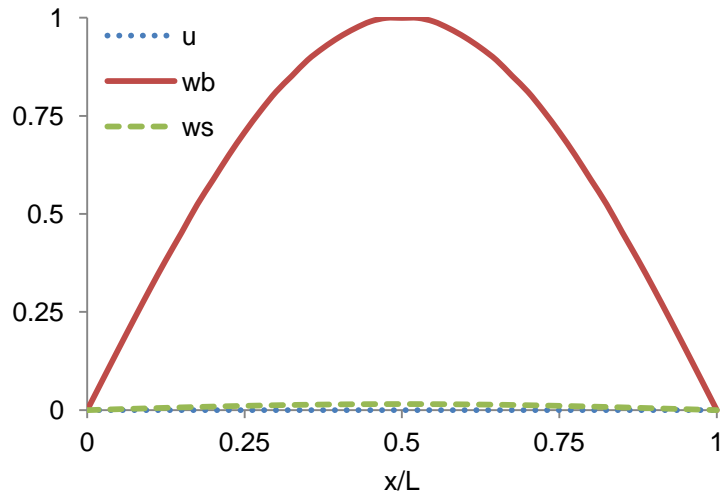
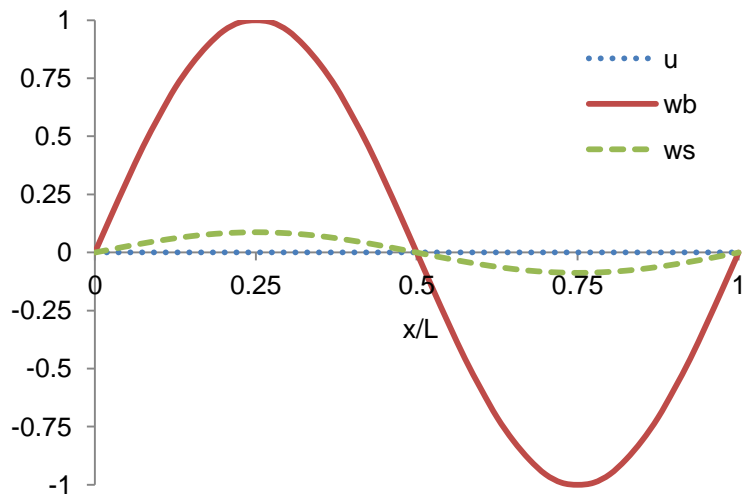


Figure 6: Variation of the non-dimensional critical buckling loads of a simply-supported anti-symmetric angle-ply  $[\theta / -\theta]$  composite beam with respect to the fiber angle change (Material IV with  $L/h = 15$ ).

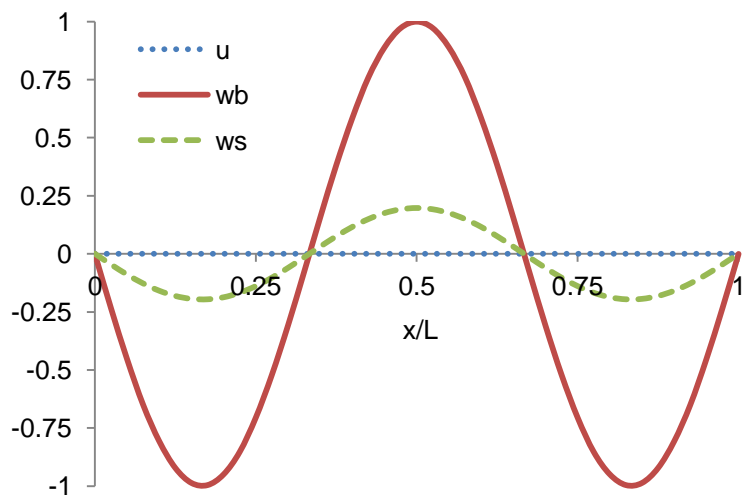




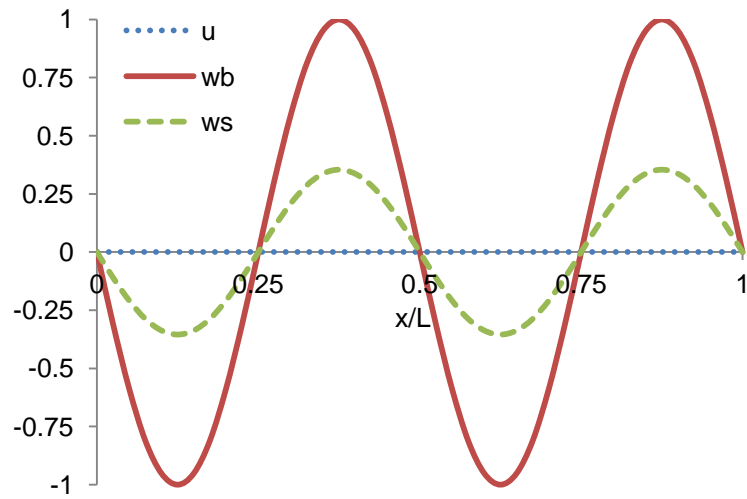
a. Fundamental mode shape  $\omega_1 = 0.9078$ .



b. Second mode shape  $\omega_2 = 3.5255$ .



c. Third mode shape  $\omega_3 = 7.5850$ .



d. Fourth mode shape  $\omega_4 = 12.7587$

Figure 7: Vibration mode shapes with the axial and flexural components of a simply-supported composite beam with the fiber angle  $45^\circ$

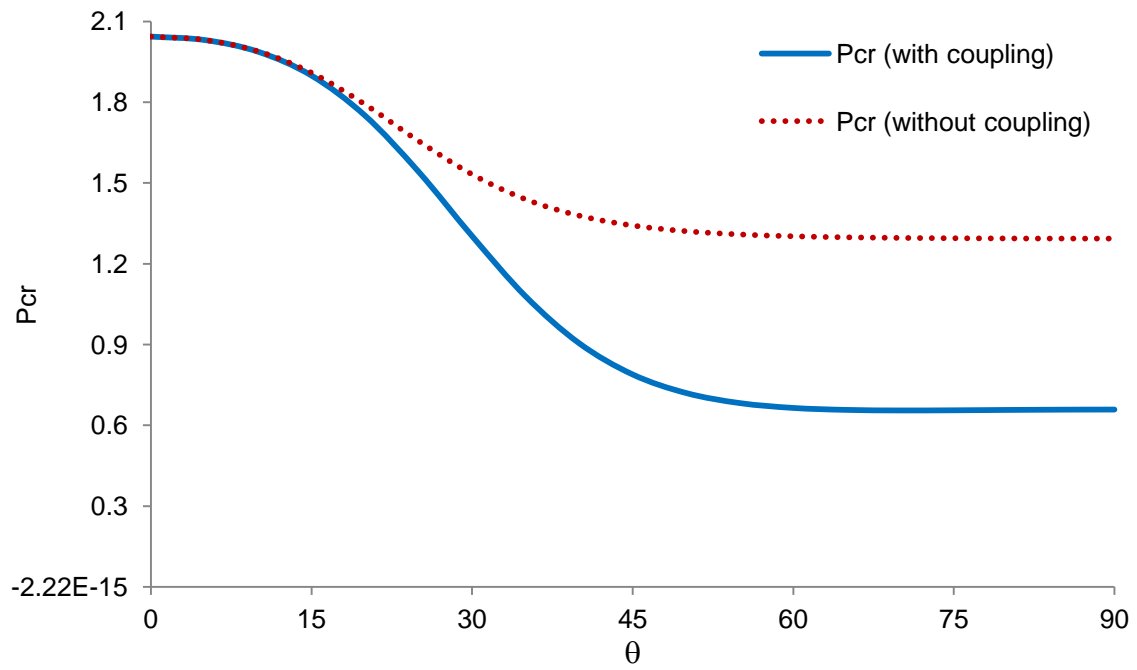
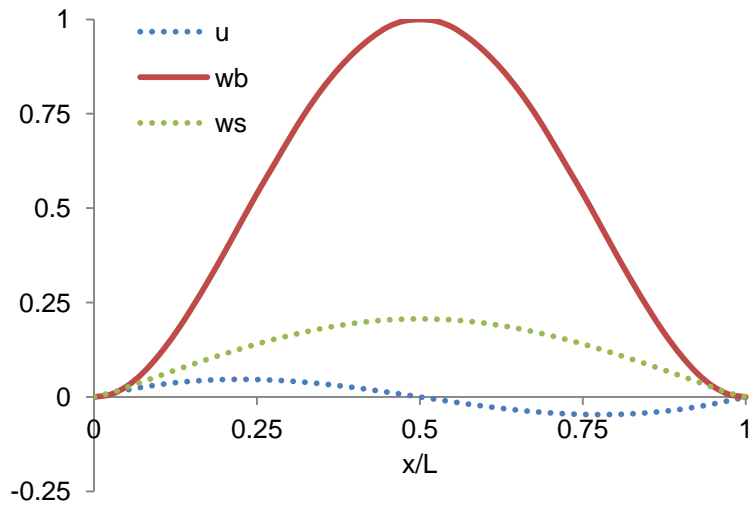
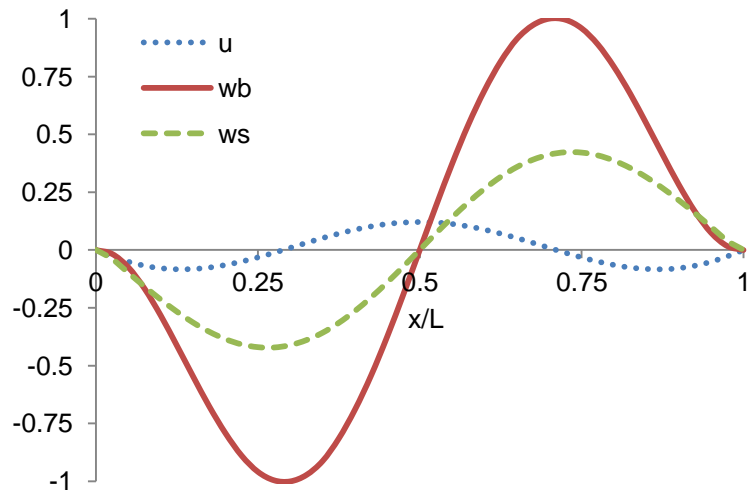


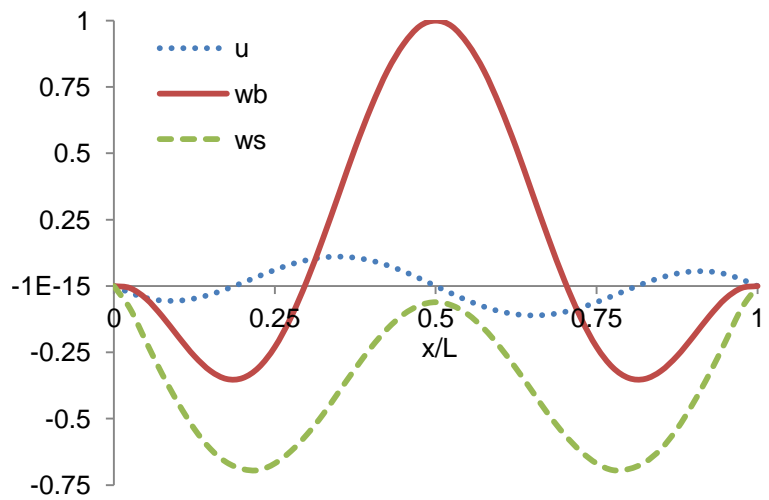
Figure 8: Variation of the non-dimensional critical buckling loads of a clamped-clamped unsymmetric  $[0/\theta]$  composite beam with respect to the fiber angle change (Material IV with  $L/h = 15$ ).



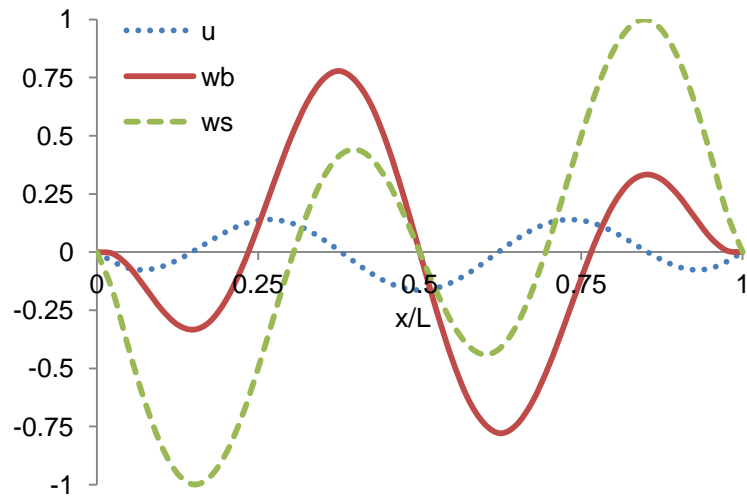
a. Fundamental mode shape  $\omega_1 = 2.859$ .



b. Second mode shape  $\omega_2 = 7.400$ .

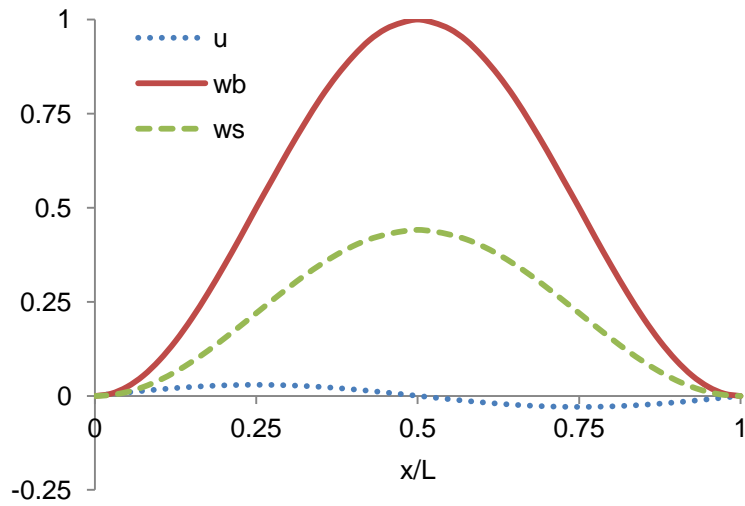


c. Third mode shape  $\omega_3 = 13.071$ .

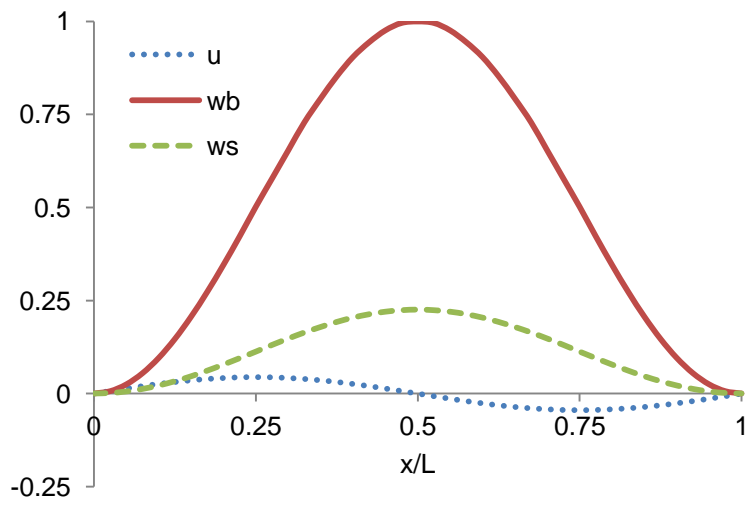


d. Fourth mode shape  $\omega_4 = 19.975$

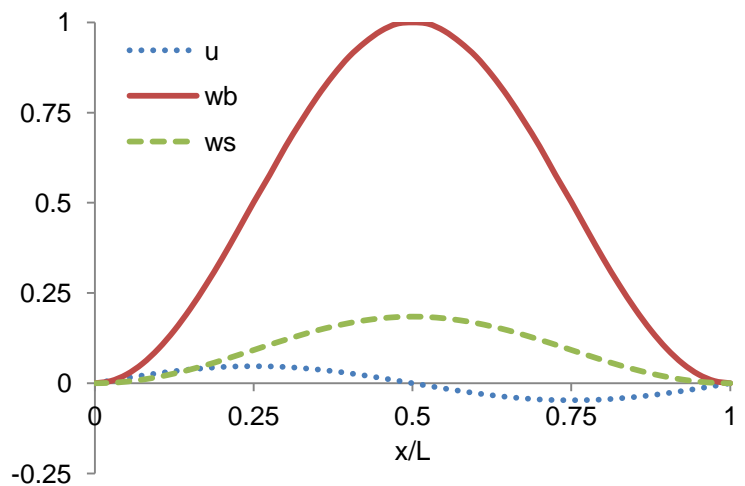
Figure 9: Vibration mode shapes with the axial and flexural components of a clamped-clamped composite beam with the fiber angle  $60^\circ$ .



a.  $P_{cr} = 1.3028$  with the fiber angle  $30^\circ$ .



b.  $P_{cr} = 0.7888$  with the fiber angle  $45^\circ$ .



c.  $P_{cr} = 0.6585$  with the fiber angle  $90^\circ$ .

Figure 10: Buckling mode shapes with the axial and flexural components of a clamped-clamped composite beam with the fiber angles  $30^\circ$ ,  $60^\circ$  and  $90^\circ$ .